International Journal of Adhesion & Adhesives 48 (2014) 210–216

Contents lists available at ScienceDirect

International Journal of Adhesion & Adhesives

journal homepage: www.elsevier.com/locate/ijadhadh

An infrared thermoelastic stress analysis investigation of single lap shear joints in continuous and woven carbon/fiber epoxy composites

Rami Haj-Ali [a], Rani Elhajjar [b,*]

[a] School of Mechanical Engineering, Faculty of Engineering Tel-Aviv University, Ramat-Aviv, Israel
[b] Department of Civil Engineering and Mechanics, University of Wisconsin-Milwaukee Milwaukee, WI, USA

ARTICLE INFO

Article history:
Accepted 30 June 2013
Available online 10 October 2013

Keywords:
Bonded joints
Composites
Thermoelastic stress analysis
Thermography
Infrared

ABSTRACT

A full-field thermoelastic stress analysis infrared method is used to study the damage initiation and progression in prepreg uni-tape and woven carbon fiber/epoxy composite single lap joints. Two loading schemes are studied to detect the damage initiation in these joints. In the first scheme the loading is monotonically increased with cyclic loading performed at the holding times. In the second scheme, the loading is increased gradually and then decreased, followed by cyclic loading at the holding time. The thermoelastic stress analysis infrared measurements show that both methods are capable of predicting the onset of damage at the bonded joint. The observed measurements indicate non self-similar crack growth or non-uniform crack extension along the bondline. Microstructural analysis is performed at the locations where damage is believed to have occurred for specimens extracted before final failure. The investigation confirms the capability of this method to capture early stages of damage in bonded joints.

1. Introduction

Engineering aircraft structures with composite materials require a detailed knowledge of durability and damage tolerance of individual structural components, especially in bonded joints due to the importance of initial manufacturing conditions. Issues such as the quality of the adhesive at the time of application, the surface preparation of the adherends, and the final void content are all known to affect the quality of the joint. Traditional mechanical testing methods using extensometers and strain gauges of composite joints may only measure linear load-deformation responses to failure, giving no indication of overload or failure initiation. They are also local measurements that are expensive to install and maintain over long periods of time. Non-destructive full-field real-time evaluation tools offer a significant refinement over traditional mechanical tests, such that failure initiation of critical components can be detected and identified early. Failure progression after initiation of damage in fiber-reinforced polymer joints is not well understood, especially for considerations of fatigue reliability after damage initiation. Different experimental methods and techniques, such as radue life of fiber-riography, photoelasticity, acoustic emission, and thermography, have been applied to investigate the fatigeinforced plastics (FRP). Bakis et al. [1] related the residual strength, stiffness, and fatigue life to corresponding damage states obtained from photoelastic coating and thermal emission experiments for graphite/epoxy laminates subjected to fully reversed fatigue loads. They observed the damage initiated around the hole for quasi-isotropic and orthotropic laminates; they also noted that matrix cracking and delamination patterns were different in both cases due to the interaction between adjacent plies. Compared with photoelastic data, the thermal emission was more sensitive to the minute deformations near the fracture paths in the surface plies. Swain et al. [2] investigated the effect of interleaves on the damage mechanisms and residual strength of notched composite laminates subjected to axial fatigue loading. They described the effect of interleaving in carbon epoxy laminates with normalized stiffness versus normalized life curves by examining residual strength and evaluated delamination by using X-ray radiography and dye-penetration. Although they were able to use traditional methods such as stiffness and strength in a quantitative measure of cumulative damage, the X-ray radiography results showed matrix cracking, delamination, and other damage mechanisms in a qualitative manner. Brien et al. [3,4] investigated damage and failure of angle ply laminated composites at or near the free edge by using X-ray radiography and optical methods. They investigated laminates using 3D Finite Element Analysis (FEA) for each configuration, looking at in-plane shear and transverse normal stresses as indicators of matrix cracks in off-axis plies. Microscopy and X-ray radiography were applied on straight coupons of AS4/350-6 graphite epoxy laminates to qualitatively validate the 3D FEA

* Corresponding author.
E-mail addresses: rami98@eng.tau.ac.il (R. Haj-Ali), elhajjar@uwm.edu (R. Elhajjar).

0143-7496/$ - see front matter © 2013 Elsevier Ltd. All rights reserved.
http://dx.doi.org/10.1016/j.ijadhadh.2013.09.013

models for load-life fatigue behavior. Using dye-enhanced X-ray radiography and microscopy, Lessard [5] investigated the effect of ply orientation on the initiation and progression of damage for the compress.

Studies have shown that the Thermoelastic Stress Analysis Infrared (TSA-IR) based technique is a powerful tool for evaluating damage in many applications with fiber reinforced polymeric materials. For example, in Dulieu-Smith et al. [6], a T-joint was investigated using TSA and correlated to a finite element analysis. Finger joints in pultruded glass-reinforced plastic (GRP) profiles were also investigated and a calibration process based on the quasi-isotropic surface layer were used [7]. The approach was also applied on a double-butt strap joint configuration of pultruded materials [8]. The results illustrate the potential to use TSA for bonded joint especially if separate calibrations can be obtained for the different regions in the bonded joint. Lin and Rowlands [9] used a complex-variable formulation involving conformal mappings to determine the individual stress components in composites. For damage in composites, Mackin and Roberts [10] tracked static damage progression in ceramic matrix composites using TSA-R on double-edge notched specimens. Bremond and Potet [11] also illustrated the advantages of TSA-IR as a non-destructive method. Kageyama et al. [12] suggested a damage threshold approach based on 3D FEA and used TSA-IR with linear elastic fracture mechanics to measure the crack propagation in notched carbon/epoxy laminates. An IR based method was also proposed and used to track the damage in [$\pm$45] and [0/90] type graphite/epoxy laminates by Lohr et al. [13]. In their experiment, the measured temperature was seen to decrease as the number of cycles increased due to cracking in the epoxy surface layer. El-Hajjar and Haj-Ali [14,15] proposed a technique to measure the sum of the direct strains on the surface of a thick section and orthotropic composites using the TSA-IR signal obtained from the surface of the specimen. Their method was verified experimentally and compared favorably with FE simulations of notched and cracked coupons. This method was used to verify damage studies in thick-section composite materials considered by Kilic and Haj-Ali [16,17]. Several studies have also investigated the use of TSA-IR to evaluate mixed-mode stress intensity factors of anisotropic laminates [15,18]. Wei et al. [19] used TSA-IR with stochastic Markov Chains to characterize the fatigue damage in composite laminates and they proposed a method to predict the S–N curve.

The single lap joint geometry due to the multiaxial stresses generated in the critical areas has been traditionally used to investigate possible changes in design to improve static and fatigue performance. It is also a common design detail in various bonded structures. In many cases FEA is used to investigate the stress distribution differences within the bondline for alternative joint geometries to better understand the effect of geometry on joint performance. For example, Zeng et al. [20] developed a wavy composite lap joint as an alternative to traditional lap joints or adhesive joint geometries with tapered edges to avoid the load eccentricity and the associated singular peel stresses at the joint ends. The wavy lap joint resulted in compressive peel stresses at the joint ends that altered the failure progression so there was no indication of damage initiation before final failure. A comparison of the wavy lap joint with the traditional lap joint showed crack initiation from the load/displacement relationship and visual inspection of cracks. Avila et al. [21] used an FEA method to make correlations between stress distributions in the wavy lap joints and the single lap joints made from E-glass/epoxy composites. They noticed a 41% higher load carrying capacity for the wavy lap joints over the conventional single-lap joints attributed to a more uniform stress field with the existence of compressive normal stresses in the wavy lap joint. Fessel et al. [22] showed significant improvements in overall joint strength for the reverse-bent joint over the traditional lap shear joint for several steel alloy substrates with different overlap lengths. They used FEA to evaluate stress distributions within the bond and discussed potential improvements of joint strength by modifying joint geometries to achieve more uniform stress distributions instead of highly localized stresses at the joint ends. Da Silva and Adams [23] compared basic double lap geometries with an inside tape and adhesive fillet design with various resins using experimentally determined failure loads and FEA to evaluate the internal stress distributions due to combined temperature and mechanical loads using titanium and carbon fiber composites. Campilho et al. [24] investigated joint efficiency using a parametric FEA study of internal stress distributions for different overlap lengths, plate thickness, and stacking sequences of single lap joints. The experimental part of their study focused mostly on ultimate failure stresses of the joints instead of failure initiation. Borsellino et al. [25] showed some evidence of capturing stabilization by investigating changes in failure (adhesive/cohesive) mechanisms with extended curing times as viewed by surface inspections of failed single lap joints. FEA was used to evaluate internal stress distributions, and the experimental evaluation was based on mechanical testing (flexural modulus, ultimate failure stresses, or impact resistance). Cheuk and Tong [26] studied the damage failure modes in lap joints in the presence of precracks. They proposed analytical methods to predict failure using maximum stresses and critical strain energy release rates.

Initial testing results on lap joints using TSA-IR with acoustic emission verifications was presented by Haj-Ali et al. [27] showed how TSA can be an effective technique in determining the onset of damage. In this study, we present an expanded view of their tests and focus on the full-field thermoelastic stress analysis infrared method (TSA-IR), specifically how to interpret the TSA-IR signal showing damage initiation and progression in prepreg uni-tape and woven carbon fiber/epoxy composite single lap joints. Two loading schemes are studied to detect the damage initiation in these joints. Microstructural analysis is performed at the locations where damage is believed to have occurred for specimens before final failure and complete failure of the bondline.

2. Thermoelastic stress analysis method

TSA-IR was applied on composite single lap joints to investigate material behavior in two joint types. The overall goal was to characterize damage evolution with an emphasis on detecting failure initiation. Progression of damage is linked to spatial small temperature changes in composite single lap shear joints. The motivation of focusing the TSA-IR testing for initiation on the bondline can be explained through an FEA stress analysis of a typical lap joint (Fig. 1). The typical behavior in such a joint is the large concentration of shear and peeling stresses at either end of the lap shear joint. Note that the area of the highest stresses is closest to the bondline fillet.

The thermoelastic stress analysis theory is based on the first and second thermodynamic laws. The thermoelastic relationship for reversible and adiabatic thermodynamic events can be expressed as [28]:

$$\rho C_\varepsilon \frac{dT}{T} = \left[\frac{\partial C_{ijkl}}{\partial T}(\varepsilon_{kl} - \alpha_{kl}\Delta T) - C_{ijkl}\left(\alpha_{kl} + \Delta T \frac{\partial \alpha_{kl}}{\partial T}\right)\right] d\varepsilon_{ij} \quad (1)$$

where ρ is the material density, C_ε the specific heat for constant deformation, T is the temperature, C_{ijkl} is the elasticity tensor, α_{kl} the thermal expansion coefficient tensor, and ε_{kl} the strain tensor. In the TSA-IR method, during cyclic loading and the presence of reversible adiabatic conditions, an infrared detector measures an un-calibrated TSA-IR signal that is dependent on the material and surface properties. In this discussion we refer to the TSA-IR signal

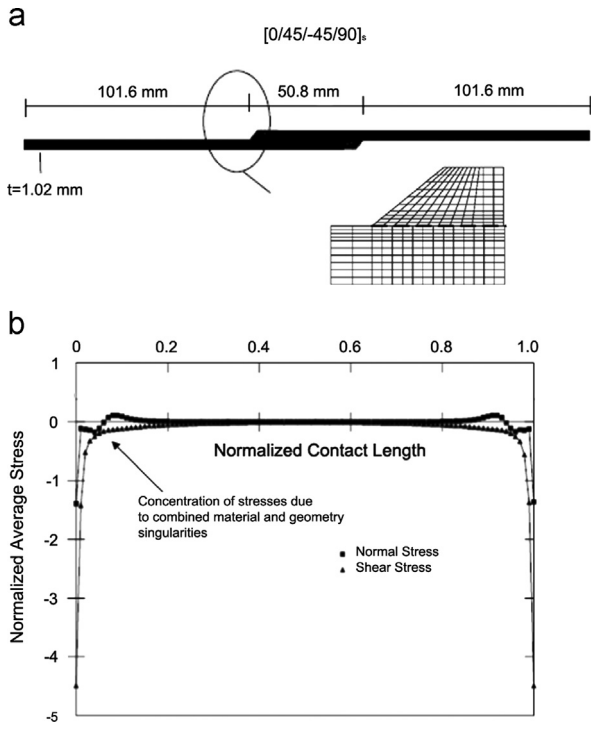

Fig. 1. Single-lap shear joint (a) Joint detail and (b) peel and shear stresses along bondline.

as S. This signal can be linearly related to the radiant photons emitted due to a surface temperature change $S \propto \frac{dT}{T} \propto \Delta\sigma$. For isotropic materials having temperature independent modulus and thermal expansion coefficients, the TSA-IR signal is related to the first invariant of the stress, $\Delta\sigma$ through a calibration constant, k_σ [14]:

$$\Delta\sigma = k_\sigma S \tag{2}$$

Thus, for the resin-rich fillet region, one expects the TSA-IR response to be directly proportional to the first invariant of stress and is representative of the stress conditions at that location. For the orthotropic material in the adherends, typically the stress invariant is not enough to characterize the behavior and the TSA-IR response observed is directly related to the in-plane strains where:

$$k_\varepsilon = \frac{C_{33}}{C_{11}C_{33} + C_{12}C_{33} - 2C_{13}^2} k_\sigma \tag{3}$$

where the constants, C, are orthotropic stiffness constants. k_ε is the TSA-IR strain constant relating the sum of the in-plane strains to the TSA-IR signal [14]:

$$\Delta\varepsilon_{\alpha\alpha} = k_\varepsilon S \quad \alpha = 1, 2 \tag{4}$$

The constant, k_ε can be directly obtained experimentally by using biaxial strain gages oriented along the material directions in unnotched coupons. The coupons are tested at various loading frequencies (1–30 Hz) and at different mean stress levels.

3. Experimental method

The quasi-isotropic composite laminates tested consisted of IM7 carbon fiber/Epoxy with eight plies in uni-tape and woven form. The resin layer used for the bonded lap-joints is an epoxy based (FM300K; Cytec Engineered Materials, Tempe, Arizona, USA) adhesive with an approximate thickness of 0.2 mm [29]. Typical properties of the uni-tape composite are shown in Table 1. A thermoelastic stress analysis infrared-based (TSA-IR) measurement system (DeltaTherm DT1500; Stress Photonics, Madison, Wisconsin, USA) was

Table 1
Typical Unidirectional material properties of IM7/epoxy composite lamina [29].

	Unidirectional	Woven (Plain weave)
Axial Modulus, GPa	164.0	85.0
Transverse Modulus, GPa	12.0	80.0
Axial Tension Strength, F1t (MPa)	2724	1090
Transverse Tension Strength. F_{2t} (MPa)	64	945

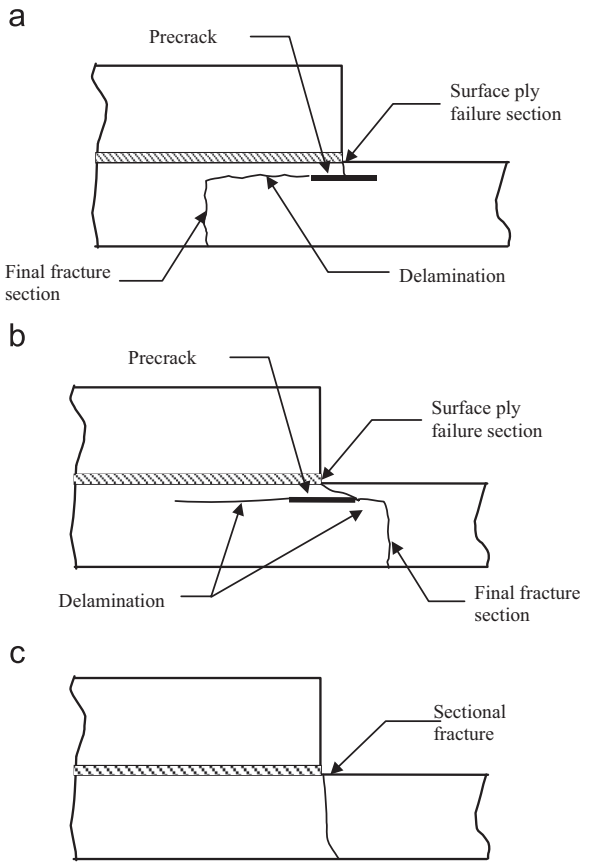

Fig. 2. Typical Failure Modes in Bonded Joints [26].

used to acquire the thermal measurements. This system has an infrared array detector synchronized with the applied cyclical loading in order to measure the transient thermoelastic effect and filter out the IR emissions not associated with the material strain energy releases. The infrared detector acts as a transducer that converts the incident radiant energy into electrical signals. A lock-in analyzer (a type of signal-processing unit) extracts the thermoelastic information from detector's output signal by using the reference signal from the loading device. The TSA-IR system uses the reference signal to reject most non-stress related thermal emissions. The DeltaTherm has a thermal resolution of approximately 1 mK. The applied load signal is used to integrate synchronized TSA images that correspond to peak values of loading. The integration of the captured images is a temporal smoothing process performed over a specified period. This study used a period of 1–2 min. The sinusoidal loading was applied using an MTS 810 (Materials Testing Systems, Minnesota, USA) servo-hydraulic test system with a 22.2 kN (50 kip) capacity. Fig. 2 shows the areas of interest in this study and the possible failure modes in

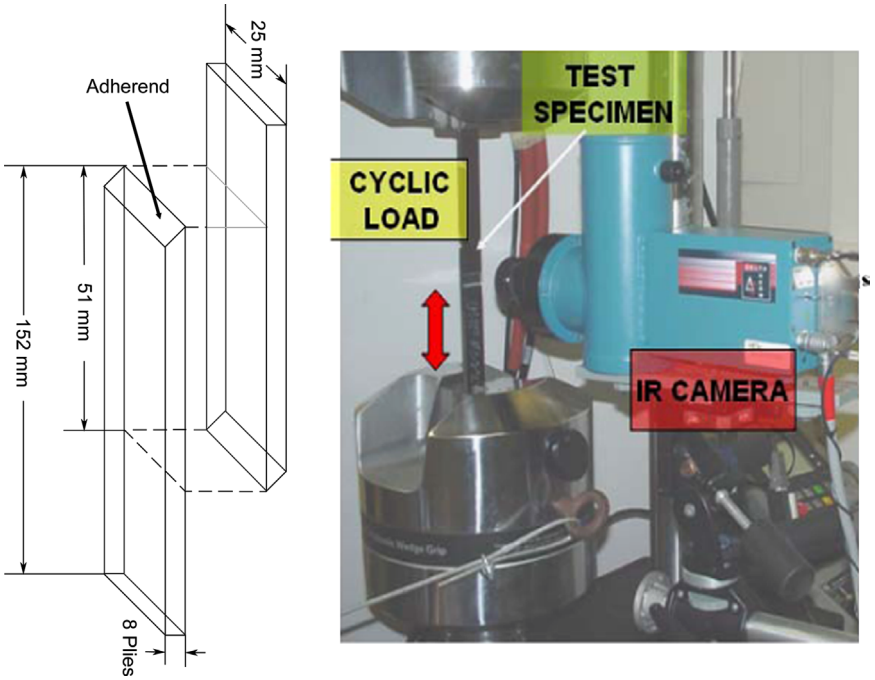

Fig. 3. Details of adhesive joint layer and TSA-IR test setup.

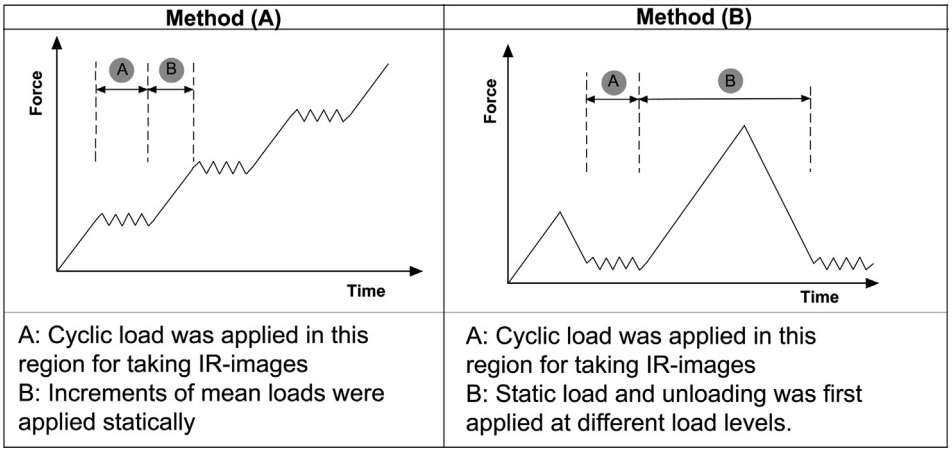

Fig. 4. TSA-IR Test Methods. Method-A: a static load step is applied, followed by constant amplitude cyclic loading (Damage Progression Approach). Method-B: a static load is applied and unloaded followed by cyclic loading at a pre-specified load and cyclic load amplitude (Crack Initiation Approach).

the specimen. A schematic of the specimen geometry and the TSA setup details in the critical region are shown in Fig. 3. Two loading protocols termed Method-A and Method-B were applied in the proposed experiment to detect damage initiation of the lap shear joints (Fig. 4). The load levels are determined by first determining the failure load of a sacrificial joint using quasi-static load levels (i.e. specimens not part of the TSA tests). Once this load is established the load is gradually increased from zero and the hold cycles depending on the observed TSA signals. The idea is to get holds for a minimum of 3 observations. In Method-A, the load is applied monotonically and paused for 1–2 minutes to acquire the TSA measurements. During this time, a small cyclic incremental load is applied at approximately 3 Hz and coupled with the TSA-IR measurements. In Method-B, once the applied load has reached a desired level, the loading is reversed to a small mean load for a short duration, in which a cyclic load is applied to be coupled with the TSA-IR measurement. The process continues by increasing the load magnitudes, followed by applied cyclic loading that can be repeated until ultimate failure is reached. A series of 6 specimens were tested using Methods A and another 6 specimens in Method B. The specimens were divided between unidirectional and woven specimens. The rationale behind the two approaches was to use Method-A for damage progression and Method-B to detect initiation. It should be mentioned that Method-B was time consuming and can be hard to automate due to the need to process each result to determine that initiation has occurred. The advantage of Method-B lies in its ability to detect damage after unloading the joint. This method was also intended to prevent additional damage to the joint due to the added cyclic loading. In addition, Method-B allows additional testing to be combined, e.g., CT-scans, X-ray, and photo-microscope tests. Failure initiation was defined in this experiment as a stress drop at points on the external edge of the bond.

4. Results and discussion

Initiation in both Method-A and Method-B is defined as a distinct drop in the stress concentration at the bondline observed

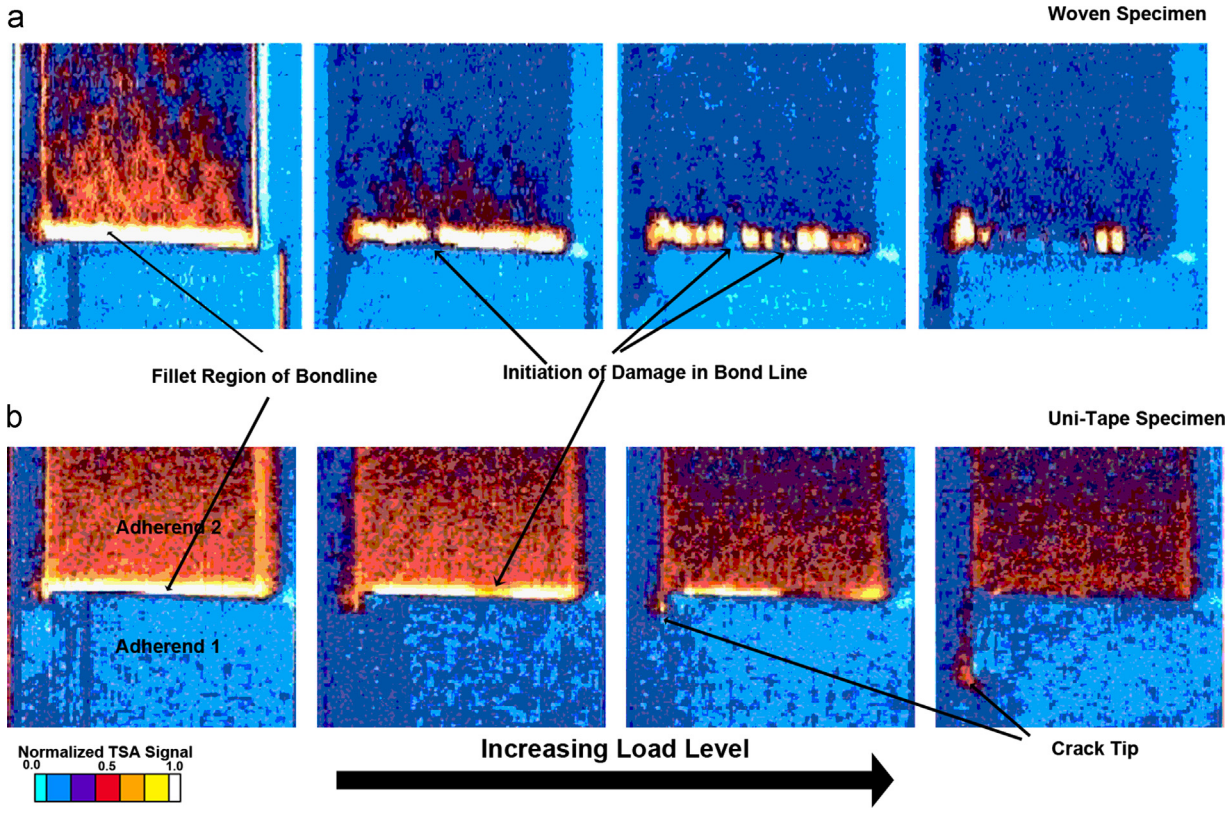

Fig. 5. Progression of failure in single-lap joints using Method-A. (a) Woven specimens: loads are between 0.9 and 19.6 kN and (b) Uni-tape specimens: the loads are between 4.4 and 14.2 kN.

from the TSA-IR measurements. The representative behavior is shown in Fig. 5 for the woven and uni-tape specimens. Note that adhesive failure was not observed and most failures occurred in the adherends. For the woven specimens, it is interesting to note the continuous stress concentration in the external bondline present at a mean load of 0.9 kN and how the TSA-IR observed line is diminished with increased loading up to 19.6 kN. We believe this result is due to the fracture of the fillet at different locations along the bond edge. As the mean load level is increased, the damage coalesces and the debonding front moves within the bond and is no longer noticeable from the IR surface inspection. The TSA-IR emissions are still visible at the crack front when observed from the specimen side. The TSA-IR images shown are normalized with respect to the maximum signal for each specimen. The loading amplitude was not altered during the test and was held constant. The fillet material due to the resin-rich area has a higher thermal response than the carbon-epoxy adherend materials. Discontinuity in the TSA response for the woven specimen was observed as early as 7.8 kN, which indicates that the failure near bondline may not be uniform and the developing crack occurs in a non self-similar manner. Note that failures observed occurred in the adherends and not in the adhesive layer. For the lap joints made from the uni-tape specimens, the TSA-IR response from the fillet region is much more localized at the fillet region and shows much more uniformity in the adherend region compared with the TSA-IR response from the woven specimens. The woven specimens had the tendency to show increased TSA-IR response due to the crimp in the adherend's woven structure. The lack of interference from the woven microstructure allows the crack front to be more easily identified in the uni-tape specimen. Using the Method-B approach where the cycling is dropped to levels lower than the highest load achieved typically results in longer test times. The Method-B results on show the ability to identify damage near the bondline after dropping the mean load levels. This is the case likely to be encountered in service when the part is overloaded and an inspection is performed at lower stress levels. In this research, we have shown that this is possible, but we have not quantitatively identified the stress levels at which this occurs. This is seen in Fig. 6 with the higher emissions occurring with increased loading of the mean stress levels.

Several specimens (one for each material and method) were preserved after noticeable damage initiation occurred and were taken for further investigation using destructive sectioning with photo-microscopy. The major assumption in the proposed testing technique is once a noticeable TSA-IR damage detection has occurred in the region near the bondline, damage within the joint area should be visually evident. One specimen was removed from each group (4 total) from testing prior to ultimate failure once the TSA-IR showed that initial failure might have occurred. This process allowed for marking of the specimens at the locations where the suspected failure initiation occurred. Prior to sectioning the specimens for micrographic inspection, each specimen was ultrasonically inspected for evidence of macroscopic flaws (e.g., delaminations greater than 1/4″ diameter). Each specimen was then sectioned and potted in preparation for micrographic inspection. Potted specimens were machined down to points near the marked TSA-IR initiation flaw points by using coarse grit paper. At this point specimens were polished down to the flaw points while being checked frequently for indications of cracking. For the unidirectional specimen evidence of micro-cracking in the adherends was significant with only some microcracks observed in the adhesive region (Fig. 7). This cross-section is the side view from the unidirectional specimen shown in Fig. 5 thus showing the matrix cracking as a possible source for the increased IR emissions.

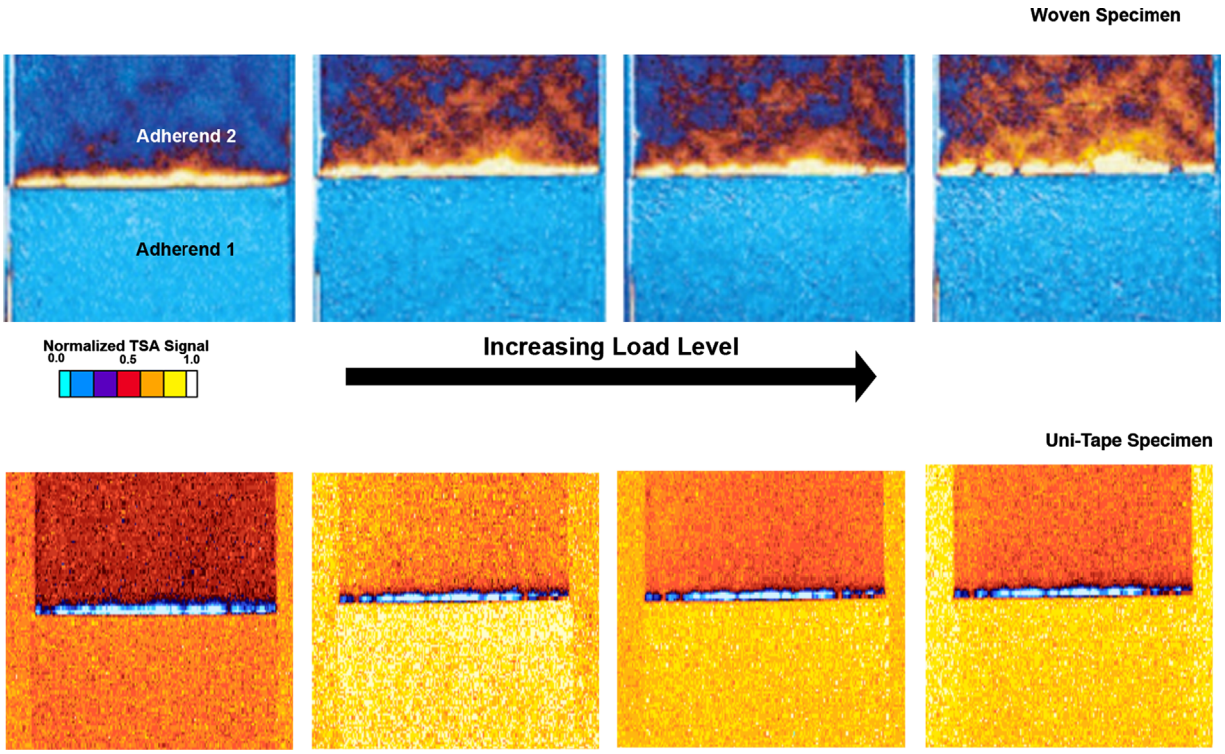

Fig. 6. Early stages of crack formation and damage initiation in a single lap shear joint made from woven and uni-specimens tested with Method B.

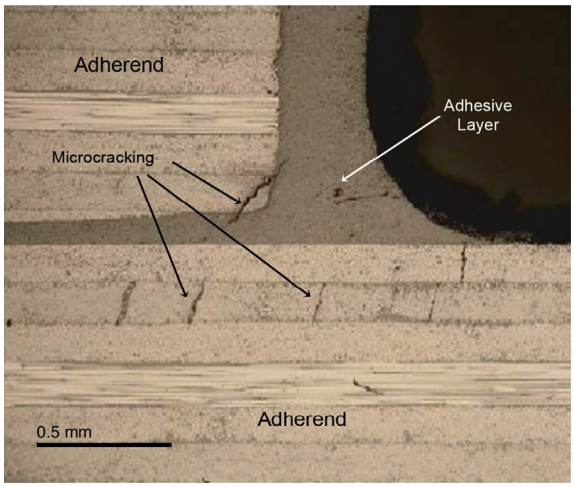

Fig. 7. Micrograph showing damage near adherend termination in single lap shear specimen before final failure as indicated from TSA-IR indication of damage.

These local failures may result in load redistribution in the joint causing the drops in the TSA-IR signal seen along other regions in the bondline.

5. Conclusions

The TSA-IR results result in confirming and shedding new light on the non-self-similar damage growth in bonded joints. The results confirm the finite element analysis results and the widely held belief showing that the largest shear and peel stresses occur near a very small region at the termination point of the adherend in the single lap shear specimen. Direct interpretation of the TSA-IR emissions into stress and strain components requires the careful development of calibration constants for distinct regions involved in the bonded joint. The results presented allow us to correlate the TSA emissions to failure in the specimens by showing higher TSA-IR response near the advancing crack front when using Method A. Micrographic testing after indications of damage from the TSA-IR signal and before final failure shows that a change in the TSA-IR signature can be correlated to damage largely in the adherends with limited cracking in the adhesive. The TSA-IR emissions from the woven specimens result in a qualitatively higher thermal signal emitted from the stresses near the crimp regions in the woven materials. This spatial region in the unidirectional specimens points to a relatively smaller region when compared to the woven specimens. The infrared response as measured using TSA-IR in both Methods A and B show that failure initiation can be defined as the formation of discontinuities near the external bondline of the single lap shear joint. This results in non self-similar damage growth. Method A and B are both able to capture these behaviors but Method B is more time-consuming due to the need to reduce the loading. The results show that structures in practice maybe inspected after overloads or damage events with low amplitude cycles to investigate the quality of the joints. However, field application of this method requires overcoming additional challenges such as acceptable load levels, frequencies and stressing methods.

Acknowledgments

This research was partially supported by a grant from the German-Israel Foundation for Scientific Research (GIF) to the first author (contract number 1166-163.10). We thank Dr. Marjorie Piechowski, University of Wisconsin-Milwaukee for assisting in editing the paper. Lockheed Martin Aeronautics Company for providing the test specimens. Shane Johnson and Bo-Siou Wei for help in performing the experiments.

References

[1] Bakis C, Yih H, Stinchcomb W, Reifsnider K. Damage initiation and growth in notched laminates under reversed cyclic loading. ASTM Special Technical Publication. 1012; 1989. p. 66–83.

[2] Swain R, Bakis C, Reifsnider KL. Effect of interleaves on the damage mechanisms and residual strength of notched composite laminates subjected to axial fatigue loading. Composite Materials: Fatigue and Fracture 1993;4:66–83.

[3] O'Brien TK. Local delamination in laminates with angle ply matrix cracks: Part 2. Delamination fracture analysis and fatigue characterization. Composite Materials: Fatigue and Fracture 1993;4:507–38.

[4] O'Brien TK, Hooper SJ. Local delamination in laminates with angle ply matrix cracks, part I: tension tests and stress analysis. ASTM Special Technical Publication. 1156; 1993. 491.

[5] Chang FK, Lessard LB. Damage tolerance of laminated composites containing an open hole and subjected to compressive loadings. I: analysis. Journal of Composite Materials 1991;25(1):2–43.

[6] Dulieu-Smith J, Quinn S, Shenoi R, Read PJCL, Moy SSJ. Thermoelastic stress analysis of a GRP tee joint. Applied Composite Materials 1997;4(5):283–303.

[7] Boyd S, Dulieu-Barton J, Rumsey L. Stress analysis of finger joints in pultruded GRP materials. International journal of adhesion and adhesives 2006;26(7):498–510.

[8] Boyd S, Dulieu-Barton J, Thomsen OT, Gherardi A. Development of a finite element model for analysis of pultruded structures using thermoelastic data. Composites Part A: Applied Science and Manufacturing 2008;39(8):1311–21.

[9] Lin S, Rowlands R. Thermoelastic stress analysis of orthotropic composites. Experimental Mechanics 1995;35(3):257–65.

[10] Mackin TJ, Roberts MC. Evaluation of damage evolution in ceramic-matrix composites using thermoelastic stress analysis. Journal of the American Ceramic Society 2000;83(2):337–43.

[11] Bremond P, Potet P. Lock-in thermography: a tool to analyze and locate thermomechanical mechanisms in materials and structures. In: Proceedings of the International Society for Optics and Photonics on aerospace/defense sensing, simulation, and controls; 2001. p. 560–6.

[12] Kageyama K, Ueki K, Kikuchi M. Fatigue damage analysis of notched carbon/epoxy laminates by thermoelastic emission and three dimensional finite element methods. In: Proceedings of international conference on composite materials–VII; 1989. p. 380–5

[13] Lohr D, Enke N, Sandor B. Analysis of fatigue damage evolution by differential infrared thermography. Dynamic Failure 1987:169–74.

[14] El-Hajjar R, Haj-Ali R. A quantitative thermoelastic stress analysis method for pultruded composites. Composites Science and Technology 2003;63(7):967–78.

[15] Haj-Ali R, Wei BS, Johnson S, El-Hajjar R. Thermoelastic and infrared-thermography methods for surface strains in cracked orthotropic composite materials. Engineering Fracture Mechanics 2008;75(1):58–75.

[16] Kilic H, Haj-Ali R. Elastic-degrading analysis of pultruded composite structures. Composite Structures 2003;60(1):43–55.

[17] Kilic H, Haj-Ali R. Progressive damage and nonlinear analysis of pultruded composite structures. Composites Part B: Engineering 2003;34(3):235–50.

[18] Lin S, Feng Z, Rowlands R. Thermoelastic determination of stress intensity factors in orthotropic composites using the J-integral. Engineering Fracture Mechanics 1997;56(4):579–92.

[19] Wei BS, Johnson S, Haj-Ali R. A stochastic fatigue damage method for composite materials based on Markov chains and infrared thermography. International Journal of Fatigue 2010;32(2):350–60.

[20] Zeng Q, Sun C. Fatigue performance of a bonded wavy composite lap joint. Fatigue and Fracture of Engineering Materials and Structures 2004;27(5):413–22.

[21] Avila AF, Bueno PO. An experimental and numerical study on adhesive joints for composites. Composite structures 2004;64(3):531–7.

[22] Fessel G, Broughton J, Fellows N, Durodola J, Hutchinson A. Evaluation of different lap-shear joint geometries for automotive applications. International Journal of Adhesion and Adhesives 2007;27(7):574–83.

[23] da Silva LF, Adams RD. Techniques to reduce the peel stresses in adhesive joints with composites. International Journal of Adhesion and Adhesives 2007;27(3):227–35.

[24] Campilho R, De Moura M, Domingues J. Modelling single and double-lap repairs on composite materials. Composites Science and Technology 2005;65(13):1948–58.

[25] Borsellino C, Calabrese L, Di Bella G, Valenza A. Comparisons of processing and strength properties of two adhesive systems for composite joints. International Journal of Adhesion and Adhesives 2007;27(6):446–57.

[26] Cheuk PT, Tong L. Failure of adhesive bonded composite lap shear joints with embedded precrack. Composites Science and Technology 2002;62(7–8):1079–95.

[27] Haj-Ali R, Koon RSE, Johnson S. Infrared thermography for failure initiation and progression in composite lap shear joints. Paper presented at the 9th International Fatigue Congress. Atlanta GA, May 14–19; 2006.

[28] Potter R, Greaves L. The application of thermoelastic stress analysis technique to fibre composites. Proceedings of SPIE 1987:134–46.

[29] HexPly® 8552 Epoxy matrix (180 °C/356 °F curing matrix); 2012 [accessed 01.02.13].